Occurrence of sapphirine-bearing granulites from Kothuru, Eastern Ghats Mobile Belt: implications on ultra-high temperature metamorphism

Saurabh Singh[1,*], Divya Prakash[1], Chandra Kant Singh[1], Vedika Srivastava[1], Manoj Kumar Yadav[2], Pradip Kumar Singh[1] and Manish Kumar[1]

[1]Centre of Advanced Study in Geology, Banaras Hindu University, Varanasi 221 005, India
[2]Centre of Advanced Study in Geology, Lucknow University, Lucknow 226 007, India

In this study, we present evidence for the stable coexistence of sapphirine + quartz and the compositional characteristics of the sapphirine-bearing granulites from Kothuru in the Eastern Ghats Mobile Belt (EGMB), India. The study area is an integral part of the Precambrian terrane in the western part of EGMB and is characterized by the granulite facies rocks comprising mainly of pelitic granulites such as charnockites, enderbites, leptynites, khondalites and gneisses, and sapphirine–spinel–quartz-bearing rocks. The chemistry of the minerals present in the assemblage has been examined using the electron probe micro analyser to infer their occurrence and distribution in various reaction textures observed during the petrographic study. The peak and post-peak history of the sapphirine-bearing granulites of Kothuru section have been constrained in the NCKFMASHTO system showing decompressional *P–T* path of high-grade metamorphic rocks through the intersection of the isopleth contours of various mineral phases present. The proposed *P–T* path with a steep isothermal decompression retrograde trajectory may be attributed to the over-thrust processes. The results obtained from the petrographic study of the mineral assemblages along with their textural relationship, mineral chemistry, especially Fe^{3+}/Fe^{Total} ratio and pseudosection modelling reveal that the studied segment has arrested promising ultra-high temperature metamorphic signatures and is tectonically distinct from those reported in the adjacent areas.

Keywords: Granulites, mineral chemistry, pseudosection modelling, reaction textures, sapphirine-bearing, ultra-high temperature metamorphism.

THE Eastern Ghats Mobile Belt (EGMB), India, is a polycyclic granulite terrane, which due to its ultra-high temperature (UHT) has elicited great interest among researchers[1]. It serves as a window to study the lower continental crustal processes and offers a potential tool for obtaining an integrated geodynamic picture of the region[2–5]. Sapphirine is a complex silicate mineral found in high-temperature metamorphic rocks or xenoliths with abundant aluminium and magnesium content. When it occurs in stable coexistence with quartz (i.e. sapphirine + quartz), this is one of the diagnostic features of UHT metamorphism[6]. The evidence of these diagnostic features of UHT metamorphism has localized occurrences in the granulite facies of rocks[7]. They represent an extreme tectonothermal event that took place in the lower crust, which may be attributed to collision followed by prolonged suturing (clockwise pressure–temperature (*P–T*) path) of the EGMB with the Indian subcontinent.

We identified a hitherto unknown locality of sapphirine–spinel granulites that contain spinel/sapphirine + quartz in an area around Kothuru in the western part of the EGMB. Isochemical pseudosections of the Mg–Al-rich metapelites were plotted to infer the peak *P–T* condition and stability field of different mineral assemblages for bulk composition of the rock samples. A textural study in accordance with the breakdown of sapphirine and garnet resulting in symplectites of various minerals was performed to shed light on the crustal evolution of the high-grade metamorphic rocks.

Geology of the study area

The study area (Kothuru, 82°34′26″E and 18°08′53″N) is situated around 120 km northwest of Visakhapatnam in Andhra Pradesh, India. It is an integral part of the EGMB comprising essentially of high-grade metamorphic terrane occurring all along the eastern coast of India, stretching from Ongole in the south to Cuttack in the north[8,9]. The EGMB can be longitudinally subdivided into four zones from west to east: western charnockite zone (WCZ), western khondalite zone (WKZ), central migmatite zone (CMZ) and eastern khondalite zone (EKZ) (Figure 1 *a*)[8,10]. The regional structural trend of the EGMB is NE–SW,

*For correspondence. (e-mail: saurabhpaliwal7@gmail.com)

which swings slightly to N–S and NNW–SSE near the southern part. Conspicuously, at the northern end, near the Mahanadi valley, the trend sharply changes to ESE–WNW and E–W[1].

The study area falls in the WCZ and WKZ, lithologically characterized by granulite facies rocks. These rocks have undergone various phases of deformation along with simultaneous and subsequent metamporphism. The localized occurrence of sapphirine–spinel–quartz-bearing rocks trending N 30°E can be observed in relatively thin bands associated with charnockite, enderbite, khondalites, and at few places with the migmatized granulites (Figure 1 *b*). Garnet-free sapphirine–spinel–quartz granulites are also extensively present. The marker bands of the sapphirine granulites in the study area are characterized by greyish-coloured granulites having a bluish tint of the cordierite-rich matrix, along with elongated grains of spinel, ilmenite/magnetite and garnet.

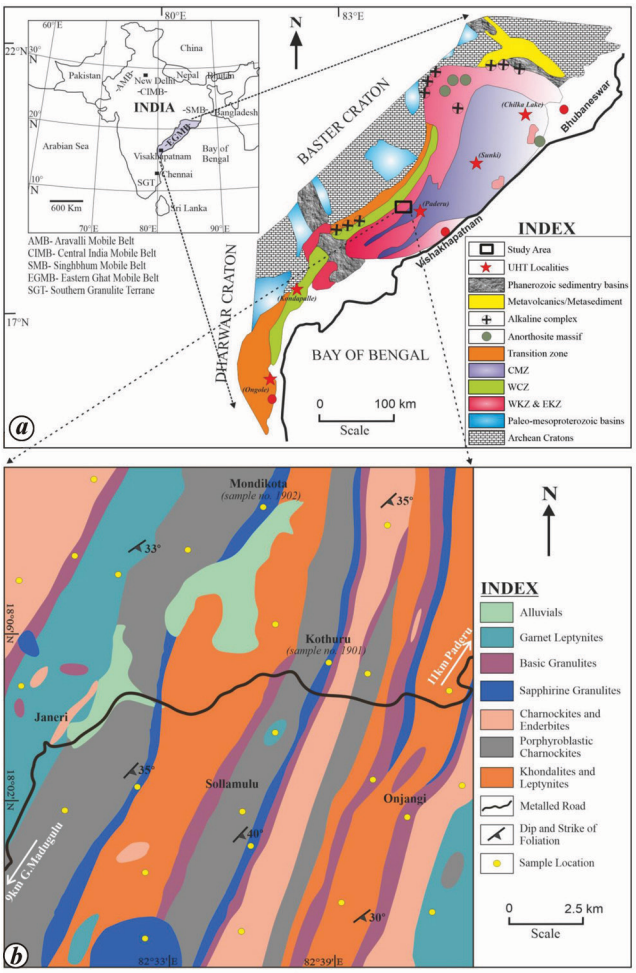

Figure 1. ***a***, Lithological map of the Eastern Ghats Mobile Belt (EGMB), India (modified after Ramakrishnan *et al.*[8]). WCZ, Western charnockite zone; WKZ, Western khondalite zone; CMZ, Central migmatite zone; EKZ, Eastern khondalite zone. ***b***, Geological map of the area around Kothuru, Visakhapatnam District, Andhra Pradesh, India.

Textural relations and interpretation of metamorphic reactions

The excellent textural relations preserved in the form of symplectites, coronas and other reaction textures in the sapphirine-bearing granulites are described in this section. Minerals present in the sapphirine-bearing granulites include sapphirine, spinel, garnet, orthopyroxene, sillimanite, quartz, K-feldspar, cordierite and biotite. At the thermal peak of metamorphism, temperature and pressure were so high that most of the earlier history has been lost. Staurolite and muscovite are completely absent. However, the relicts of biotite, sillimanite, orthopyroxene in garnet, sapphirine and spinel minerals are useful tools for inferring the pre-history of the thermal peak of metamorphism. Coarse porphyroblasts of garnets$_1$ (Grt$_1$) are formed during the early episodes of granulite facies metamorphism. The presence of inclusions of biotite, quartz and sillimanite within megacrystic garnet and K-feldspar may be ascribed to the following prograde reaction (Figure 2 *a*):

$$\text{Biotite} + \text{sillimanite} + \text{quartz} = \text{garnet}_1 + \text{K-feldspar} + H_2O. \quad (1)$$

Unusual grain contact of spinel/sapphirine with quartz was present in a number of samples (Figure 2 *b* and *c*), which suggests that spinel/sapphirine and quartz were in equilibrium during the thermal peak of metamorphism. In the later stages, sapphirine formed a rim around spinel and spinel was isolated from quartz. This early corona texture may be related to the following reactions:

$$\text{Spinel} + \text{quartz} = \text{sapphirine}_{2:2:1}. \quad (2)$$

$$\text{Spinel} + \text{sillimanite} + \text{quartz} = \text{sapphirine}_{7:9:3}. \quad (3)$$

The textural evidences indicate that spinel was associated with quartz, and later reacted with quartz to form different reaction coronas due to change in metamorphic conditions. On the basis of textural evidences, it can be inferred that spinel is first retrograded to sapphirine, followed by spinel + sillimanite, orthopyroxene + sillimanite and spinel + cordierite + orthopyroxene + sillimanite. Spinel with exsolution textures occurs in the matrix of cordierite and quartz. The exsolved spinel was mantled by sillimanite.

Medium-grained, typically xenoblastic garnet$_2$ (Grt$_2$) occurs usually as granular aggregates around coarser grains of garnet$_1$ or orthopyroxene (Figure 2 *d*). These garnets contain inclusions of sapphirine and spinel. Sometimes garnet is separated from the inclusions of spinel by sillimanite or sapphirine (Figure 2 *d*), which suggests the following reactions:

$$\text{Spinel} + \text{quartz} = \text{garnet}_2 + \text{sillimanite}. \quad (4)$$

$$\text{Spinel} + \text{quartz} = \text{sapphirine} + \text{garnet}_2. \quad (5)$$

The first generation of orthopyroxene$_1$ (Opx$_1$) is medium- to coarse-grained, xenoblastic to subidioblastic, highly fractured, isolated from any type of symplectite and coronas and contains inclusions of quartz, sillimanite, spinel, sapphirine, biotite and K-feldspar (Figure 2 *e*). The retrograde biotite occurs either along the crack or on the outer margin of orthopyroxene$_1$. The second generation of orthopyroxene$_2$ (Opx$_2$) is feeble to strongly pleochroic, medium to fine-grained and occurs in the different coronas and granular aggregates in the symplectites (Figure 2 *f*). Medium-grained orthopyroxene$_2$ is associated with sapphirine and spinel separated by sillimanite, suggesting the following reactions:

$$\text{Spinel} + \text{quartz} = \text{orthopyroxene}_2 + \text{sillimanite}. \quad (6)$$

$$\text{Sapphirine} + \text{quartz} = \text{orthopyroxene}_2 + \text{sillimanite}. \quad (7)$$

As the temperature decreases due to cooling and pressure being released during exhumation, the sapphirine–spinel–quartz assemblage becomes incompatible. The sapphirine is now rimmed by cordierite in spite of orthopyroxene, sillimanite and quartz (Figure 2 *g*). Thus, cordierite is formed and sapphirine–spinel–cordierite becomes the compatible assemblage. The reactions involved in the formation of cordierite are

$$\text{Spinel} + \text{quartz} = \text{cordierite}. \quad (8)$$

$$\text{Sapphirine}_{2:2:1} + \text{quartz} = \text{cordierite}. \quad (9)$$

At the end of the last phase of uplifting, sapphirine and spinel became incompatible with quartz and cordierite. Water activity (fluid) dominates over the CO_2 fluid because hydrous minerals like biotite and cordierite begin to react to produce different types of symplectites (Figure 2 *h*). The coronas do not form due to non-refractory behaviour of the minerals. Garnet which is in the early stage of retrogression, ultimately became unstable due to the following reaction:

$$\text{Garnet}_1 + \text{K-feldspar} + H_2O = \text{cordierite} + \text{biotite} + \text{quartz}. \quad (10)$$

Mineral chemistry

The chemical analyses of minerals were carried out using an electron probe micro analyzer (EPMA; CAMECA SX-Five instrument) at the DST-SERB National Facility, Department of Geology, Banaras Hindu University, Varanasi, India. Table 1 lists the representative microprobe analyses of various minerals from Kothuru.

Sapphirine

This is highly aluminous with Al_2O_3 content ranging from 60.98 to 62.36 wt%. Sapphirine is also fairly rich in iron with FeO content up to 10.38 wt%, substantial amounts of ferrous (up to 0.452 wt%) and ferric content (up to 0.076 wt%), characterizing the sapphirine-bearing pelitic granulites. The X_{Mg} values calculated on 10-oxygen basis for sapphirine range from 0.749 to 0.788, with negligible variations between core and rim data. The sapphirine occurs as rims around porphyroblasts of spinel in the stoichiometric (Mg, Fe) O : Al_2O_3 : SiO_2 relation 2 : 2 : 1. The X_{Mg} values for sapphirine rims within garnet are found to be slightly higher than those within cordierite.

Orthopyroxene

Orthopyroxene grains show noticeable variations in Al_2O_3 content. They are characterized by a decrease in Al_2O_3

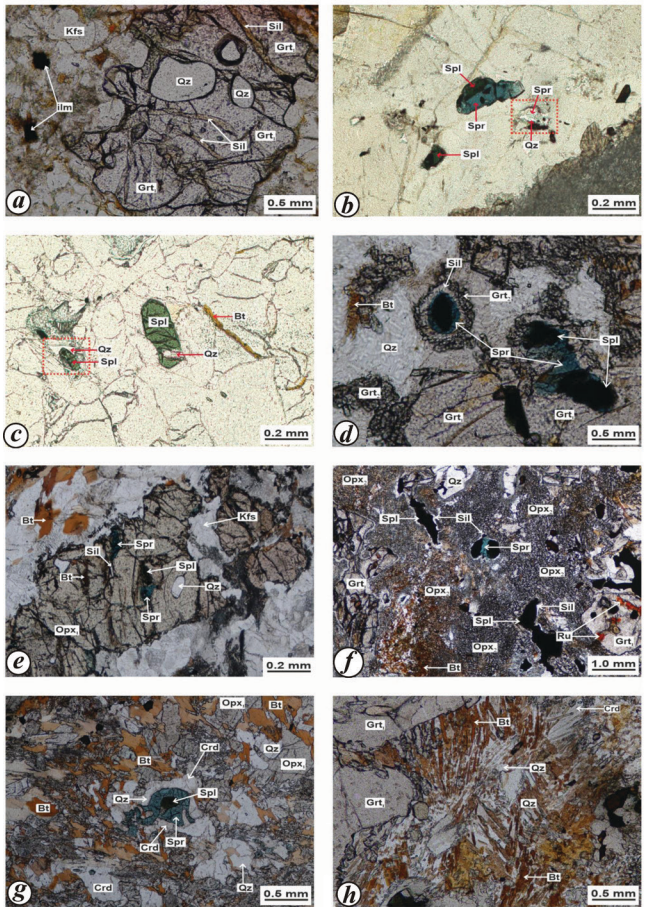

Figure 2. Photomicrographs illustrating the textural relationship in sapphirine–spinel-bearing granulite under plane polarized light: ***a***, inclusions of biotite, quartz and sillimanite within megacryst of garnet, indicating the prograde metamorphic stage; ***b***, unusual grain contact of sapphirine with quartz in equilibrium, suggesting the thermal peak of metamorphism; ***c***, rare occurrence of spinel and quartz in contact at equilibrium, indicating the thermal peak of metamorphism; ***d***, reaction corona of garnet$_2$ (outer rim) and sillimanite (inner rim) separating sapphirine (blue) from quartz; ***e***, coarse-grained orthopyroxene$_1$ with inclusions of quartz, sillimanite, spinel, sapphirine, biotite and K-feldspar; ***f***, orthopyroxene$_2$ associated with sapphirine and spinel separated by thin rims of sillimanite; ***g***, sapphirine$_{2:2:1}$ reacts with quartz to form cordierite; ***h***, formation of symplectites of biotite and cordierite at later stages during exhumation.

Table 1. Electron microprobe analyses of the minerals

Spot no.	35/1	41/1	50/1	54/1	26/1	60/1	71/1	75/1	55/1	56/1	62/1	63/1	13/1
Sample no.	1901	1901	1902	1902	1901	1901	1902	1902	1901	1901	1902	1902	1901
	C	R	C	R	R	C	I	I	I	I	C	R	I
Mineral	Grt_1	Grt_1	Grt_2	Grt_2	Opx_1	Opx_1	Opx_2	Opx_2	Spr	Spr	Spr	Spr	Bt
SiO_2	40.61	40.04	39.97	39.85	47.36	47.98	50.43	49.69	12.29	12.55	12.49	12.45	38.35
Al_2O_3	22.29	22.58	22.18	22.32	8.70	9.43	6.89	6.87	62.36	62.02	61.32	60.98	12.70
TiO_2	0.03	0.00	0.00	0.00	0.16	0.10	0.08	0.07	0.00	0.04	0.11	0.00	4.27
FeO	22.92	22.81	23.21	24.12	20.82	19.67	19.62	19.33	8.59	8.99	10.38	10.37	10.43
MnO	0.43	0.39	0.41	0.47	0.27	0.14	0.14	0.25	0.01	0.00	0.05	0.05	0.11
MgO	14.17	13.92	13.32	12.85	21.92	21.27	23.40	22.41	15.48	15.61	14.87	15.42	18.42
CaO	0.18	0.17	0.46	0.24	0.07	0.10	0.10	0.04	0.01	0.00	0.00	0.00	0.00
Na_2O	0.02	0.01	0.01	0.01	0.06	0.01	0.05	0.03	0.01	0.01	0.00	0.00	0.08
K_2O	0.05	0.00	0.01	0.00	0.04	0.00	0.00	0.00	0.00	0.00	0.00	0.00	9.38
Total	100.70	99.93	99.59	99.86	99.41	98.70	100.70	98.68	98.76	99.22	99.21	99.26	96.93
O basis	12	12	12	12	6	6	6	6	10	10	10	10	22
Si	3.016	2.996	3.011	3.005	1.767	1.786	1.837	1.846	0.745	0.758	0.760	0.757	5.704
Al	1.951	1.992	1.970	1.984	0.383	0.414	0.296	0.301	4.451	4.414	4.395	4.372	2.226
Ti	0.002	0.000	0.000	0.000	0.005	0.003	0.002	0.002	0.000	0.002	0.005	0.000	0.478
Fe^{2+}	1.393	1.416	1.443	1.510	0.650	0.612	0.598	0.601	0.375	0.387	0.452	0.414	1.297
Fe^{3+}	0.031	0.012	0.019	0.012	0.000	0.000	0.000	0.000	0.060	0.067	0.076	0.114	0.000
Mn	0.027	0.025	0.026	0.030	0.009	0.004	0.004	0.008	0.001	0.000	0.002	0.002	0.013
Mg	1.568	1.552	1.495	1.444	1.219	1.180	1.270	1.241	1.397	1.405	1.348	1.398	4.084
Ca	0.014	0.014	0.037	0.020	0.003	0.004	0.004	0.002	0.000	0.000	0.000	0.000	0.000
Na	0.003	0.002	0.002	0.001	0.004	0.000	0.003	0.002	0.001	0.001	0.000	0.000	0.024
K	0.005	0.000	0.001	0.000	0.002	0.000	0.000	0.000	0.000	0.000	0.000	0.000	1.780
Total	8.01	8.01	8.00	8.01	4.04	4.00	4.01	4.00	7.03	7.03	7.04	7.06	15.61
X_{Mg}	0.530	0.523	0.509	0.489	0.652	0.658	0.680	0.674	0.788	0.784	0.749	0.772	0.759

Spot no.	30/1	31/1	51/1	8/1	15/1	45/1	39/1	68/1	70/1	7/1	20/1	38/1	24/1
Sample no.	1901	1901	1902	1902	1902	1901	1901	1902	1902	1902	1902	1901	1901
	C	R	Incl.	R	C	I	M	M	M	M	M	M	M
Mineral	Bt	Bt	Bt	Spl	Spl	Spl	Crd	Crd	Crd	Kfs	Kfs	Kfs	Ilm
SiO_2	39.40	39.93	38.93	0.08	0.16	0.25	51.60	49.79	49.39	64.73	64.47	66.22	0.08
Al_2O_3	13.34	13.53	14.14	59.66	59.32	63.86	30.76	32.57	32.87	18.42	18.23	17.61	0.00
TiO_2	4.59	4.64	5.35	0.08	0.00	0.00	0.00	0.02	0.00	0.05	0.03	0.02	48.63
FeO	6.34	5.95	4.86	28.92	30.42	22.94	2.94	3.40	3.54	0.07	0.00	0.11	45.52
MnO	0.14	0.20	0.00	0.05	0.01	0.11	0.00	0.07	0.00	0.00	0.00	0.04	0.06
MgO	20.49	20.70	20.16	9.80	8.97	12.73	12.00	11.35	13.07	0.00	0.00	0.03	2.19
CaO	0.00	0.00	0.04	0.00	0.02	0.06	0.00	0.04	0.02	0.18	0.16	0.03	0.02
Na_2O	0.21	0.19	0.42	0.00	0.01	0.02	0.14	0.04	0.03	2.55	1.08	2.79	0.01
K_2O	9.40	9.26	8.94	0.00	0.00	0.02	2.39	0.01	0.01	14.08	13.78	10.93	0.05
Total	95.78	95.85	94.91	98.60	98.90	100.00	99.82	97.28	98.94	100.09	97.74	97.78	97.12
O basis	22	22	22	4	4	4	18	18	18	8	8	8	6
Si	5.723	5.747	5.665	0.002	0.004	0.006	5.172	5.061	4.955	2.979	3.012	3.054	0.008
Al	2.284	2.295	2.425	1.945	1.942	1.984	3.634	3.902	3.888	0.999	1.004	0.957	0.000
Ti	0.502	0.502	0.585	0.002	0.000	0.000	0.000	0.001	0.000	0.002	0.001	0.001	1.916
Fe^{2+}	0.771	0.716	0.591	0.618	0.653	0.496	0.053	0.251	0.140	0.003	0.000	0.004	1.790
Fe^{3+}	0.000	0.000	0.000	0.051	0.054	0.009	0.194	0.039	0.157	0.000	0.000	0.000	0.200
Mn	0.017	0.024	0.000	0.001	0.000	0.003	0.000	0.006	0.000	0.000	0.000	0.002	0.003
Mg	4.437	4.441	4.375	0.404	0.371	0.500	1.792	1.719	1.955	0.000	0.000	0.002	0.171
Ca	0.000	0.000	0.006	0.000	0.001	0.002	0.000	0.004	0.002	0.009	0.008	0.001	0.001
Na	0.060	0.053	0.118	0.000	0.000	0.001	0.027	0.007	0.005	0.228	0.097	0.250	0.000
K	1.741	1.700	1.660	0.000	0.000	0.001	0.305	0.001	0.002	0.827	0.821	0.643	0.000
Total	15.56	15.48	15.43	3.02	3.03	3.00	11.18	10.99	11.10	5.05	4.94	4.91	4.084
$X_{Mg(or)K}$	0.852	0.861	0.881	0.395	0.363	0.502	0.971	0.873	0.933	0.777	0.887	0.719	0.079

$X_{Mg} = Mg/(Mg + Fe^{2+})$, $X_K = K/(K + Na + Ca)$; C, Core; R, Rim; I, Intermediate; M, Matrix; Incl., Inclusion.

content from core (9.43 wt%) to rim (8.70 wt%), and increase in MgO content from core (X_{Mg} 0.658) to rim (X_{Mg} 0.652), irrespective of their association with garnet or sapphirine in the pelitic granulite. The high Al_2O_3 values in the core suggest the development of the mineral during the peak *P–T* condition of metamorphism, while lower Al_2O_3 values towards the rim indicate the later cooling stage of metamorphism. $Orthopyroxene_1$ (9.43–8.70) is

observed to be more aluminous than orthopyroxene$_2$ (6.87–6.89).

Cordierites

These are mostly dry and the most magnesian phase among all the minerals present in the rock sample, with X_{Mg} values ranging between 0.87 and 0.97. The occurrence of cordierite is in accordance with the substitution proposed by Schreyer *et al.*[11], i.e. $Si^{+} \Leftrightarrow Al^{+}$ (Na, K). However, the alkalis are almost negligible to absent[12]. The cordierites are unzoned, occurring as inclusions and intergrowth with quartz and feldspar.

Spinel

This is generally Mg spinel – hercynite and magnetite solid solutions with X_{Mg} values ranging from 0.363 to 0.502, which are less than the coexisting X_{Mg} values of orthopyroxene, sapphirine, biotite, cordierite and garnet.

Garnets

These are mainly solid solutions of almandine (46.93–64.78 mol%) and pyrope (30.62–62.64 mol%) with minor amounts of grossularite (up to 4.2 mol%) and spessartine (up to 1.7 mol%). The coexistence of garnet with orthopyroxene is sporadic on rare occasions, indicating that the assemblage garnet–orthopyroxene–cordierite could have coexisted in the same phase at some stage during the metamorphic evolution of these granulites. Garnet$_1$ (0.530–0.523) has higher X_{Mg} values than garnet$_2$ (0.509–0.489). The X_{Mg} values of sapphirine-bearing garnet range from 0.53 to 0.49. The contrast in the X_{Mg} values of garnet is due to the higher MgO content in the sapphirine-bearing garnets.

Biotites

Biotites with high TiO_2 content (4.27–5.35 wt%) characterize the sapphirine-bearing mineral assemblage of the pelitic granulite. Biotites are fairly rich in fluorine (up to 5.30 wt%) and occur in close association with aluminous orthopyroxene and cordierite, suggesting high temperatures of melting of the prograde mineral assemblage[13]. The biotites present are highly magnesian with X_{Mg} values ranging from 0.76 to 0.88.

K-feldspars

These are generally present as grains associated with orthopyroxene, sapphirine and quartz. They also occur as inclusions as well as intergrowth textures with cordierite and quartz in the matrix. Perthitic intergrowth textures occur commonly in the metapelites. The presence of high sanidine/anorthoclase in some metapelites is likely to be the result of high-temperature melting. The X_K values of K-feldspar range from 0.72 to 0.89.

Plagioclases

These are found in less abundance compared to K-feldspars in the metapelites. The X_{An} values for plagioclase have a narrow range from 0.36 to 0.37 and are mainly albitic in nature.

Ilmenite

This is found mainly in the matrix. The TiO_2 content (48.63 wt%) is slightly higher than the FeO content (45.52 wt%).

P–T pseudosection modelling

Isochemical pseudosection modelling from the average bulk composition (XRF data in wt%: Na_2O – 1.39, MgO – 10.44, Al_2O_3 – 15.7, SiO_2 – 56.3, K_2O – 2.07, CaO – 0.85, TiO_2 – 1.47, MnO – 0.09, FeO – 10.42; loss of ignition (LOI) – 0.86), to estimate the peak and post-peak (retrograde) *P–T* condition of the sapphirine-bearing granulites from the Kothuru section have been used. The XRF analysis was carried at the Birbal Sahni Institute of Palaeosciences (BSIP), Lucknow (WD-XRF; power – 3 KW, 60 kV–160 mA) to detect the elements.

The peak and post-peak history of the sapphirine-bearing granulites was constrained using the Perple_X software (version 6.8.7) from the internally consistent thermodynamic dataset and the equation of state for H_2O of Holland and Powell[14,15], which is based on the Gibbs free energy minimizations[16–19].

The *P–T* evolution of the sapphirine-bearing granulite was estimated within the pressure–temperature range 6–10 kbar and 900–1050°C respectively, based on the NCKFMASHTO (Na_2O–CaO–K_2O–FeO–MgO–Al_2O_3–SiO_2–H_2O–TiO_2–Fe_2O_3) model system. The amount of H_2O (wt%) used in the computation of the *P–T* pseudosection was approximated from the LOI value obtained in the bulk composition analysis. The thermodynamic data file hp02ver.dat was used to formulate the *P–T* pseudosection model[14] with solution models Gt(W), Opx(W), Kf, Pl(h), Sp(JH), Crd(W), melt(HP), Sapp(HP) and Bio(TCC). The obtained pseudosection shows the stability field of different mineral assemblages at possible *P–T* conditions. Based on the petrography and EPMA analysis, the minerals identified were input to Perple_X ver. 6.8.7 with their suitable end-members as pure phases, which includes garnet (alm, py, gr and spss), orthopyroxene (en

and fs), sapphirine (Spr4, Spr7 and fspr), spinel (sp, herc and usp), cordierite (crd, hcrd and fcrd), biotite (phl, ann and east), plagioclase (ab and an), K-feldspar (san and mic), silicate melt phase (fo8L, fa8L, sill8L and q8L), sillimanite (sill, ky & and) and quartz (q, trd, coe and stv). The obtained pseudosection was then contoured with the compositional modal proportion isopleths of various mineral phases, i.e. X_{Mg} sapphirine, X_{Mg} spinel, X_{Mg} cordierite, X_{Mg} biotite, X_{Mg} garnet and X_{Mg} orthopyroxene (X_{Mg} = Mg/Mg + Fe).

The *P–T* path derived from the intersection of the isopleth contours (X_{Mg} compositional values), suggests the peak mineral assemblage to be spinel–garnet–orthopyroxene–cordierite–biotite–plagioclase–sapphirine–melt–quartz–rutile at a pressure of about 9.5 kbar and temperature in excess of 980°C (Figure 3). The decompression path projected shows an abrupt release in pressure from 9.5 to 6.8 kbar, which corresponds to the exhumation of these granulites.

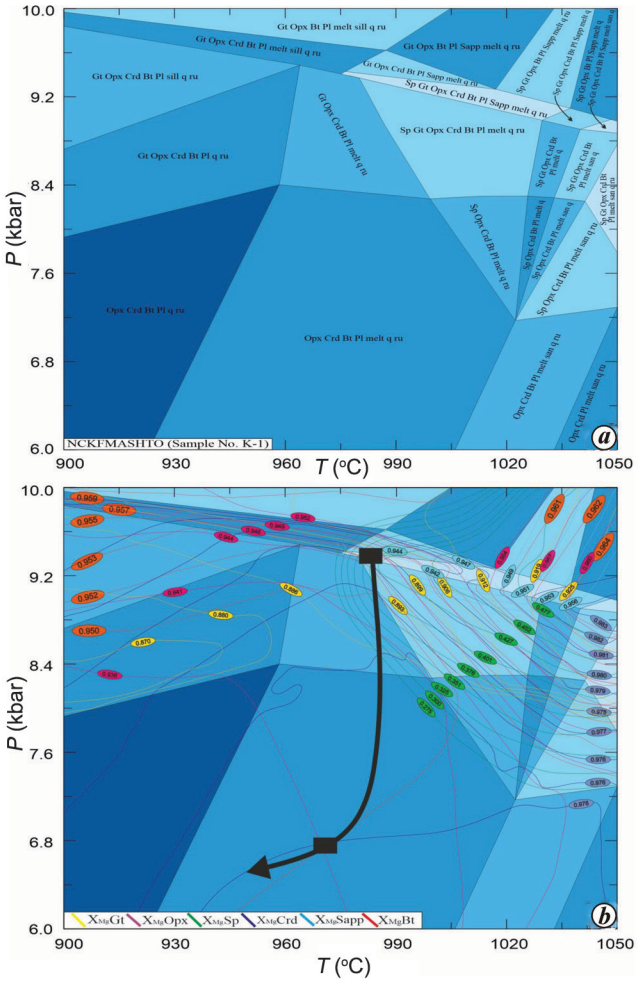

Figure 3. ***a***, *P–T* pseudosection approximation for possible stable assemblages of sapphirine–spinel-bearing granulite (sample no. 1901) in the NCKFMASHTO model system with bulk composition (in wt%) Na_2O – 1.39, MgO – 10.44, Al_2O_3 – 15.70, SiO_2 – 56.30, K_2O – 2.07, CaO – 0.85, TiO_2 – 1.47, MnO – 0.09, FeO – 10.42, loss of ignition – 0.86. ***b***, Estimated pseudosection contoured with calculated X_{Mg} isopleths and the inferred isothermal decompressional *P–T* path.

Discussion and conclusion

The stable coexistence of sapphirine and spinel with quartz in contact, and their incompatibility at later stages represented by polymineralic reaction coronas provide robust evidence that the studied granulite terrane has undergone extreme crustal metamorphism at UHT (>950°C at ~10 kbar). Several UHT localities have been reported from different parts of the EGMB by earlier workers (Figure 1 *a*) and their extent of metamorphism lies in close proximity with results obtained in terms of *P–T* condition in the present study. However, it differs in textural relations and the mechanism through which such extreme temperature and pressure have resulted. The highly aluminous orthopyroxene (with Al_2O_3 content up to 9.43 wt%) characterizes the granulites of the locality and this is found to be in accordance with other UHT belts like the Enderby Land, Antarctica (Al_2O_3 content of 8–9.5 wt%) with similar *P–T* conditions of 10 ± 1.5 kbar and 950° ± 50°C respectively[20]. The observed aluminous assemblage and *P–T* conditions of the study area are also in close correlation with the UHT models documented from the Southern Granulite Terrane of India[21,22], and in the adjacent areas of the EGMB[23]. The calculated ratio of Fe^{3+}/Fe^{Total} in sapphirine from the data obtained from the microprobe studies is significantly low (<0.3), which in turn fulfils a major criterion as the indicator of UHT metamorphism[6].

The derived *P–T* trajectory of metamorphism from pseudosection modelling for the high-grade metamorphic rocks shows the peak *P–T* condition and post-peak isothermal decompression retrograde trajectory followed by isobaric cooling (second stage of retrograde trajectory). The proposed clockwise *P–T* path with steep isothermal decompression retrograde trajectory is considered to be in favour of collision tectonics and over-thrust processes, which is also evident from the abrupt occurrence of transition zone to the west of the presented segment. In such metamorphic belts, the peak *P–T* condition (mainly pressure ranges) is often underestimated due to the dominance of widely occurring retrograde overprints in mineral assemblages and arrested reaction textures. Santosh and Kusky[24] proposed a model for the estimation of extreme *P–T* conditions associated with collision/thrust tectonics which may also be applicable in the present study, in which the heat required to balance the anhydrous mineral assemblages of various UHT occurrences from collisional belts may be derived from the asthenospheric upwelling developed due to subduction of the ridges. The present study provides evidences (petrographic, geochemical and pseudosection modelling) for the occurrence of a UHT locality which is tectonically different from those reported in the adjacent localities, suggesting an anti-clockwise *P–T*

path with primary retrograde stage of isobaric cooling. Further studies of the mineral inclusions and isotopic geochronology may help unravel the mechanism and precise timing involved in the evolution of the tectonometamorphic framework related to the UHT metamorphic belts of collisional suture.

1. Mukhopadhyay, D. and Basak, K., The Eastern Ghats belt – a polycyclic granulite terrain. *J. Geol. Soc. India*, 2009, **73**, 489–518.
2. Dasgupta, S., Bose, S. and Das, K., Tectonic evolution of the Eastern Ghats Belt, India. *Precambrian Res*., 2013, **227**, 247–258.
3. Das, K., Bose, S., Karmakar, S., Dunkley, D. J. and Dasgupta, S., Multiple tectonometamorphic imprints in the lower crust: first evidence of ca. 950 Ma (zircon U–Pb SHRIMP) compressional reworking of UHT aluminous granulites from the Eastern Ghats Belt, India. *Geol. J*., 2011, **46**, 217–239.
4. Korhonen, F. J., Brown, M., Clark, C. and Bhattacharya, S., Osumilite-melt interactions in ultrahigh temperature granulites: phase equilibria modelling and implications for the *P–T–t* evolution of the Eastern Ghats Province, India. *J. Metamorph. Geol.*, 2013, **31**, 881–907.
5. Prakash, D., Singh, D., Singh, P. C., Singh, C. K., Tewari, S., Arima, M. and Frimmel, H. E., Reaction textures and metamorphic evolution of sapphirine–spinel-bearing and associated granulites from Diguva Sonaba, Eastern Ghats Mobile Belt, India. *Geol. Mag.*, 2015, **152**, 316–340.
6. Harley, S. L., Refining the *P–T* records of UHT crustal metamorphism. *J. Metamorph. Geol.*, 2008, **26**, 125–154.
7. Dharma Rao, C. V., Santosh, M. and Chmielowski, R. M., Sapphirine granulites from Panasapattu, Eastern Ghats Belt, India: ultrahigh-temperature metamorphism in a Proterozoic convergent plate margin. *Geosci. Front*., 2012, **3**, 9–31.
8. Ramakrishnan, M., Nanda, J. K. and Augustine, P. F., Geological evolution of the Proterozoic Eastern Ghats Mobile Belt. *Geol. Surv. India*, *Spec. Publ*., 1998, **44**, 1–21.
9. Dasgupta, S. and Sengupta, P., Indo-Antarctic correlation: a perspective from the Eastern Ghats Belt. *Geol. Soc. London*, *Spec. Publ*., 2003, **206**, 131–143.
10. Nanda, J. K. and Pati, U. C., Field relations and petrochemistry of the granulites and associated rocks in the Gnjam–Koraput sector of the Eastern Ghats Belt. *Indian Miner*., 1989, **43**, 247–264.
11. Schreyer, W., Maresch, W. V. and Daniels, P., Potassic cordierites: characteristic minerals for high-temperature, very low-pressure environments. *Contr. Mineral. Petrol*., 1990, **105**, 162–172.
12. Vry, J. K., Brown, P. E. and Valley, J. W., Cordierite volatile content and the role of CO_2 in high-grade metamorphism. *Am. Mineral*., 1990, **75**, 71–88.
13. Bose, S., Das, K. and Fukuoka, M., Fluorine content of biotite in granulite-grade metapelitic assemblages and its implications for the Eastern Ghats granulites. *Eur. J. Mineral.*, 2005, **17**, 665–674.
14. Holland, T. J. B. and Powell, R., An internally-consistent thermodynamic dataset for phases of petrological interest. *J. Metamorph. Geol.*, 1998, **16**, 309–343.
15. Holland, T. J. B. and Powell, R., An improved and extended internally consistent thermodynamic dataset for phases of petrological interest, involving a new equation of state for solids. *J. Metamorph. Geol.*, 2011, **29**, 333–383.
16. Connolly, J. A. D., Multivariable phase-diagrams – an algorithm based on generalized thermodynamics. *Am. J. Sci*., 1990, **290**, 666–718.
17. Connolly, J. A. D., Computation of phase equilibria by linear programming: a tool for geodynamic modeling and its application to subduction zone decarbonation. *Earth Planet. Sci. Lett*., 2005, **236**, 524–541.
18. Connolly, J. A. D., The geodynamic equation of state: what and how. *Geochem. Geophys. Geosyst*., 2009, **10**, 1–19.
19. Connolly, J. A. D. and Petrini, K., An automated strategy for calculation of phase diagram sections and retrieval of rock properties as a function of physical conditions. *J. Metamorph. Geol.*, 2002, **20**, 697–708.
20. Harley, S. L. and Hensen, B. J., Archaean and Proterozoic high-grade terranes of East Antarctica (40–80°E); a case study of diversity in granulite facies metamorphism. *Mineral. Soc. Ser*., 1990, **2**, 320–370.
21. Tamashiro, I., Santosh, M., Sajeev, K., Morimoto, T. and Tsunogae, T., Multistage orthopyroxene formation in ultrahigh-temperature granulites of Ganguvarpatti, southern India: implications for complex metamorphic evolution during Gondwana assembly. *J. Mineral. Petrol. Sci*., 2004, **99**, 279–297.
22. Tateishi, K., Tsunogae, T., Santosh, M. and Janardhan, A. S., First report of sapphirine + quartz assemblage from Southern India: implications for ultrahigh temperature metamorphism. *Gondwana Res*., 2004, **7**, 899–912.
23. Lal, R. K., Ackermand, D. and Upadhyay, H., *P–T–X* relationships deduced from corona textures in sapphirine–spinel–quartz assemblages from Paderu, southern India. *J. Petrol*., 1987, **28**, 1139–1168.
24. Santosh, M. and Kusky, T. M., Origin of paired high pressure–ultrahigh–temperature orogens: a ridge subduction and slab window model. *Terra Nova*, 2010, **22**, 35–42.

ACKNOWLEDGEMENTS. S.S. and D.P. thank the Department of Science and Technology, New Delhi for DST-INSPIRE Fellowship (IF 180879) and DST (SERB) Research Project (P-07-704) respectively. We thank the Head, Department of Geology, Banaras Hindu University (BHU), Varanasi and the CAS programme of University Grants Commission, New Delhi at BHU for providing necessary infrastructural facilities. We also thank the anonymous reviewer for valuable suggestions that helped improve the manuscript.

Received 1 September 2021; revised accepted 19 March 2022

doi: 10.18520/cs/v122/i11/1298-1304